

PRELIMINARY VIRTUAL FLIGHT VALIDATION OF A QUAD TILT ROTOR UAV IN WIND TUNNEL

Duoneng Liu^{1, 2}, Wenkai Wang¹, Bendong Zhao¹, Xingzhi Hu¹ & Bowen Nie^{2, *}

¹ Beijing Aerohydrodynamic Frontier Research Center

² Low Speed Aerodynamic Institution, China Aerodynamic Research and Development Center

*Contact Author

Abstract

This paper focuses on a quad tilt rotor unmanned aerial vehicle (UAV) with both the ability of vertical take-off and landing (VTOL) and high speed cruise, briefly introduces the overall layout and flying mechanics, and formulates the model of flight dynamics for the three flight modes, including the VTOL mode, the conversion mode and the fixed wing mode, with one formation which takes the tilt angle of rotor as a variable. Next, the surface allocation, tilt conversion corridor and flight control law is designed, and the closed loop flight control system is constructed. At last, all the system is integrated for the virtual flight test in wind tunnel, which evaluates augmentation effect and handling performance of the control laws in three flight modes, and preliminary validates the tilt conversion corridor and its control scheme.

Keywords: unmanned aerial vehicle, quad tilt rotor, flight control law, virtual flight test, wind tunnel

1. Introduction

Research and development on the vertical take-off and landing (VTOL) aircraft have regained much attention in recent years [1, 2]. NASA and Defense Advanced Research Projects Agency (DARPA) have started programs to develop next-generation advanced VTOL aircraft [3]. NASA's VTOL unmanned aerial vehicle (UAV) named GL-10 successfully completed the transition flight tests [4]. The Japan Aerospace Exploration Agency (JAXA) has been investigating the practical applicability of VTOL aircraft as a future civil transport, and they have proposed a commuter class Quad-Tilt-Wing (QTW) aircraft [5, 6]. At the Low Speed Aerodynamic Institution of the China Aerodynamics Research and Development Center in China, a Quad Tilt Rotor (QTR) tandem wing UAV is taken as a benchmark for verification and validation of flight control laws in conversion flights.

In order to conduct conversion flight between the VTOL configuration and the fixed wing configuration, direction of the thrusts varies from 0 to 90 deg by tilting the four rotors simultaneously. The dynamics of the QTR aircraft are not stable for most wing tilt angles, and the unstable dynamic characteristics of the motions change dramatically according to the rotor tilt angles [7]. Therefore, flight control law design is thus a key factor to make sure that the QTR aircraft flies safely.

This paper summarizes the design, verification, implementation and flight test of Control Augmentation System (CAS) for a Quad Tilt Rotor (QTR) Unmanned Aerial Vehicle (UAV) in the low speed wind tunnel which has VTOL as well as high speed cruise capabilities. The control law design is based on the tilt corridor and scheduled by the tilt angle of the rotors of the QTR UAV. After being preliminarily verified in simulations, the control law is readily rapid prototyped in the flight computer and integrated with the avionic instruments including sensors and actuators. Performance of the flight control law is further verified by virtual flight tests in wind tunnel and the QTR UAV successfully achieved steady VTOL model, tilt conversion mode, fixed wing mode, and full conversion flight; that is, the QTR UAV achieved vertical take-off, accelerating transition, high speed cruise, decelerating transition, and vertical landing.

2. Flying and Handling Mechanics

2.1 Layout of the Quad Tilt Rotor UAV

As presented in Figure 1(a), the QTR UAV is a tandem fixed-wing aircraft equipped with a rotor on

each tip, which can tilt from level to vertical. There are no control surfaces on the front wing and vertical tail, except two flaperons on the rear wing driven by an actuator to deflect as elevators or split as ailerons. As shown in Figure 1(b), the four rotors are driven by brushless motors to direction A (clockwise) and B (anticlockwise) in order to cancel the counter torque as much as possible. The four motors are connected to the same linkage and driven to tilt synchronously by an actuator. Besides, the avionic system including all the sensors and actuators is located inside the fuselage.



(a) QTR UAV Benchmark

(b) Overall Layout

Figure 1 – Overall layout of the quad-tilt rotor UAV.

2.2 Flying Modes and Handling Mechanics

The motions of the QTR UAV are controlled by propellers driven by electric motors mounted at the wing tips, and aerodynamic force driven by flaperons implemented at the trailing edges of rear wings. The handling mechanics is shown in Figure 2. In VTOL mode, pitching moment is generated by the thrust difference between the fore and rear propellers, rolling moment is generated by the thrust difference between the left and right propellers, and yawing moment is generated by adjusting the clockwise and anticlockwise reaction torques of four propellers. In fixed-wing mode, pitching moment is generated by simultaneously deflecting left and right flaperons of rear wings, rolling moment is generated by the force difference between the left and right flaperons, and yawing moment is generated by force made by thrust difference between the left and right propellers. In transition mode between VTOL and fixed-wing modes, combination method of interpolating between these modes is used. Thus, the motor rate command is the sum of ones for pitching control, rolling control, yawing control and pilot throttle stick position. Similarly, flaperon command is the sum of ones for pitching and rolling control.

	pitch control	roll control	yaw control
VTOL mode	thrust difference 	thrust difference 	reaction torque
transition mode	combination of VTOL and fixed-wing modes		
fixed-wing mode	flaperons 	flaperons 	thrust difference

Figure 2 – Handling mechanics for different flight modes.

3. Modeling of Flight Dynamics

3.1 General Equations

Following a standard approach, the aircraft model is obtained from the dynamics and kinematics equations [8]. The 12th order aircraft model may thus be summarized as follows:

$$\begin{cases} \dot{V} = \frac{1}{m}F - \Omega \times V \\ \dot{\Omega} = I^{-1}(M - \Omega \times I\Omega) \\ \dot{X} = R(\Phi)V \\ \dot{\Phi} = T(\Phi)\Omega \end{cases} \quad (1)$$

where, $V = [u \ v \ w]^T$, $\Omega = [p \ q \ r]^T$, $X = [x_E \ y_E \ h]^T$, $\Phi = [\varphi \ \theta \ \psi]^T$. $R(\Phi)$ and $T(\Phi)$ denote the rotation matrixes.

The forces applied to the aircraft can be decomposed into three terms (engines thrust, gravity and aerodynamic forces):

$$\begin{aligned} F &= F_{eng} + F_g + F_a \\ &= \begin{bmatrix} (T_{fl} + T_{fr} + T_{rl} + T_{rr})\cos(\tau_w) \\ 0 \\ -(T_{fl} + T_{fr} + T_{rl} + T_{rr})\sin(\tau_w) \end{bmatrix} + R(\Phi)^T \begin{pmatrix} 0 \\ 0 \\ mg \end{pmatrix} + q \cdot S_{ref} \begin{bmatrix} C_{xb} \\ C_{yb} \\ C_{zb} \end{bmatrix} \end{aligned} \quad (2)$$

The moment about the center of gravity G of the aircraft results from the rotors, aerodynamic actions and moment resulting from the thrust:

$$\begin{aligned} M &= M_{eng} + M_a \\ &= \begin{bmatrix} (T_{fl} - T_{fr} + T_{rl} - T_{rr})\sin(\tau_w) \cdot l_{Ty} \\ (T_{fl} + T_{fr})\sin(\tau_w) \cdot l_{Txf} - (T_{rl} + T_{rr})\sin(\tau_w) \cdot l_{Txr} \\ (T_{fl} - T_{fr} + T_{rl} - T_{rr})\cos(\tau_w) \cdot l_{Ty} \end{bmatrix} \\ &\quad + \begin{bmatrix} (M_{fl} - M_{fr} - M_{rl} + M_{rr})\cos(\tau_w) \\ 0 \\ (-M_{fl} + M_{fr} + M_{rl} - M_{rr})\sin(\tau_w) \end{bmatrix} + q \cdot S_{ref} \begin{bmatrix} C_{lb_wb} \cdot b \\ C_{mb_wb} \cdot \bar{c} \\ C_{nb_wb} \cdot b \end{bmatrix} + GA \times F_{a_wb} \end{aligned} \quad (3)$$

In formula (2) and (3), $\tau_w \in [0^\circ \ 90^\circ]$ denotes the tilt angle of rotor, l_{Ty} is the roll arm of rotor, l_{Txf} and l_{Txr} denote the front and rear pitch arm respectively, S_{ref} is the area of both wings, $[C_{xb} \ C_{yb} \ C_{zb}]^T$ denotes the coefficients of aerodynamic forces in the body fixed coordinate, $[C_{lb_wb} \ C_{mb_wb} \ C_{nb_wb}]^T$ is the coefficients of aerodynamic moments also in the body frame, b is the wing span, \bar{c} is the mean chord, GA is the length between the center of mas and the aerodynamic reference point.

The amount of force generated by the rotor is proportional to the square of its rotational speed. The rotor speed command consists of the following six parts: throttle trimming, throttle command, rotor elevator, rotor aileron, rotor rudder, and the counter torque rudder. In addition, assuming that the rotational speed dynamics of the four rotors are the same, they can all be represented by a first-order system. Therefore, the dynamic models of the four rotors can be expressed as:

$$\begin{cases} T_{fl} = k_{pro} \left\{ f_{sch} \left[\delta_{th_trim} + \frac{1}{T_{thS+1}} (\delta_{th_c} + \delta_{pwele_c} + \delta_{pwail_c} + \delta_{pwrud_c} - \delta_{anrud_c}) \right] \right\}^2 \\ T_{fr} = k_{pro} \left\{ f_{sch} \left[\delta_{th_trim} + \frac{1}{T_{thS+1}} (\delta_{th_c} + \delta_{pwele_c} - \delta_{pwail_c} - \delta_{pwrud_c} + \delta_{anrud_c}) \right] \right\}^2 \\ T_{rl} = k_{pro} \left\{ f_{sch} \left[\delta_{th_trim} + \frac{1}{T_{thS+1}} (\delta_{th_c} - \delta_{pwele_c} + \delta_{pwail_c} + \delta_{pwrud_c} + \delta_{anrud_c}) \right] \right\}^2 \\ T_{rr} = k_{pro} \left\{ f_{sch} \left[\delta_{th_trim} + \frac{1}{T_{thS+1}} (\delta_{th_c} - \delta_{pwele_c} - \delta_{pwail_c} - \delta_{pwrud_c} - \delta_{anrud_c}) \right] \right\}^2 \end{cases} \quad (4)$$

where, the speed control command is a dimensionless value from 0 to 100%, and the dimensional speed (rpm) is calculated via looking-up table; the coefficient k_{pro} and the time constant of T_{th} can be calibrated by experiments.

The flaperons are driven by digital servos, which can also be regarded as a first-order system. Deflection of the left and right flaperon is combined by the elevator and aileron commands:

$$\begin{cases} \delta_{F_l} = \frac{1}{T_aS+1} (\delta_{flelv_c} + \delta_{ftail_c}) \\ \delta_{F_r} = \frac{1}{T_aS+1} (\delta_{flelv_c} - \delta_{ftail_c}) \end{cases} \quad (5)$$

The time constant T_a is also obtained by experimental calibration.

3.2 Surface Allocation

According to flying and handling mechanics of the QTR UAV, the surface allocation scheme in each

flight mode is designed as following:

VTOL mode: while $60^\circ \leq \tau_w \leq 90^\circ$, aerodynamics resulting from the fixed-wing is neglectable. The pitch motion is controlled via differential action between the front and rear rotors. Meanwhile, the elevator surface is kept at zero, which means $K_{\delta\theta_{\tau w}} = 1$, as shown in Figure 3; The roll motion is controlled via differential action between the left and right rotors, and the yaw motion is controlled via counter torque between the clockwise and anticlockwise rotors. Besides, the aileron surface is also kept at zero, which means $K_{\delta\phi_{\tau w}} = 1$ and $K_{\delta\psi_{\tau w}} = 0$, as shown in Figure 4.

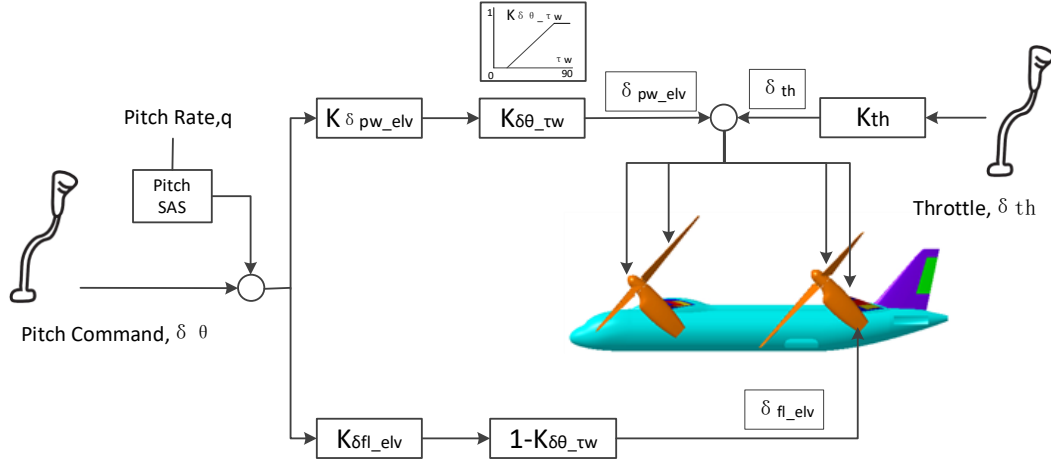


Figure 3 – Control assignment scheme for the longitudinal channel.

Fixed-wing mode: while $0^\circ \leq \tau_w \leq 30^\circ$, the fixed-wing aerodynamics plays a leading role, and the above vertical take-off and landing mode control commands are all set to zero. The pitch attitude is controlled by the elevator, the aileron controls the roll motion, and the heading is controlled via differential action between left and right rotors. As a result, $K_{\delta\theta_{\tau w}} = 0$, $K_{\delta\phi_{\tau w}} = 0$ and $K_{\delta\psi_{\tau w}} = 1$, as shown in Figure 3 and 4.

Tilt conversion mode: while $30^\circ < \tau_w < 60^\circ$, both the VTOL and the fixed-wing mode is active. Taking the tilt angle τ_w as variable, the weighting coefficients of $K_{\delta\theta_{\tau w}}$, $K_{\delta\phi_{\tau w}}$ and $K_{\delta\psi_{\tau w}}$ can be tabulated and interpolated to construct the corresponding surface allocation scheme.

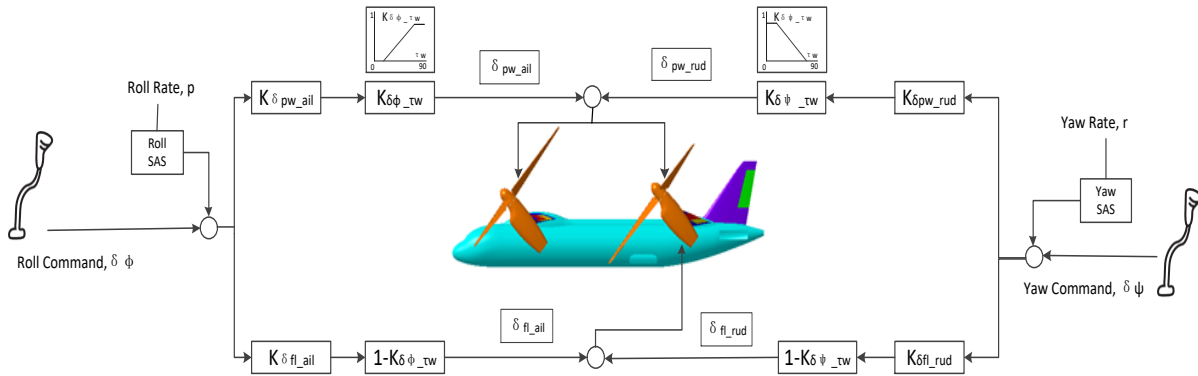


Figure 4 – Control assignment scheme for the lateral & directional channels.

3.3 Tilt Conversion Corridor

The tilt angle schedule against airspeed in conversion mode is designed based on trimming analyses of each rotor tilt angle generated from the simulation of nonlinear flight dynamics model. The corridor for the conversion schedule is determined based on angle of attack before wing stall. The trimming and analysis were carried out under the configurations of $\tau_w = [90^\circ, 80^\circ, 60^\circ, 30^\circ, 15^\circ, 0^\circ]$ respectively, as shown in Figure 5.

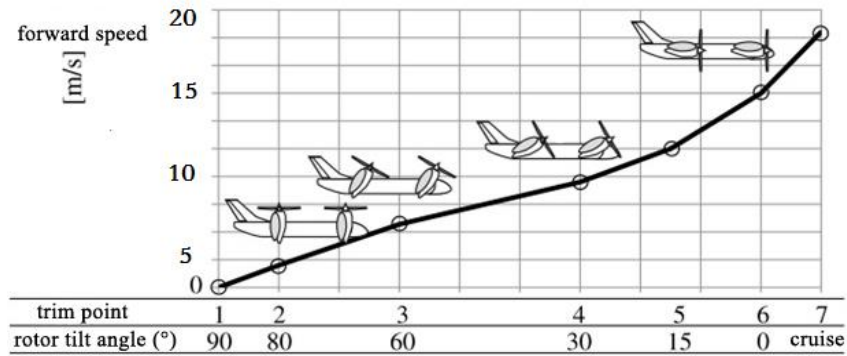


Figure 5 – Schematic diagram of the tilting corridor during transitional flight.

4. Flight Control Law

4.1 Longitudinal Channel

The longitudinal flight control law [9] is designed as a pitch angle Control Augmentation System (CAS), as shown in Figure 6. For the inner loop, pitch rate is fed back and proportional gained to improve damping ratio; In the out loop, pitch angle is fed back for a Proportional-Integral (PI) controller which aims to speed up response and decline error of the closed-loop. As a result, while placing the stick at neutral pitch position, the aircraft keeps level; pulling the stick, the aircraft noses up; pushing the stick, the aircraft noses down. The flight speed channel is controlled as a open-loop which modifies the motors' speed simultaneously via throttle.

At each trimming point of the conversion corridor, the control gains are deduced with root locus. Otherwise, the control gains are interpolated from the neighbourhood trimming points.

4.2 Lateral & Directional Channel

As presented in Figure 7, a roll angle CAS [9] is designed for the lateral channel with controller structure and manipulation mechanics similar to the longitudinal channel. However, the yaw controller is just a Stability Augmentation System(SAS). Due to the deterioration of heading sensor in wind tunnel, only yaw rate is available for feedback to improve yaw damping ratio. While placing the stick to left, the aircraft turns left, vice versa.

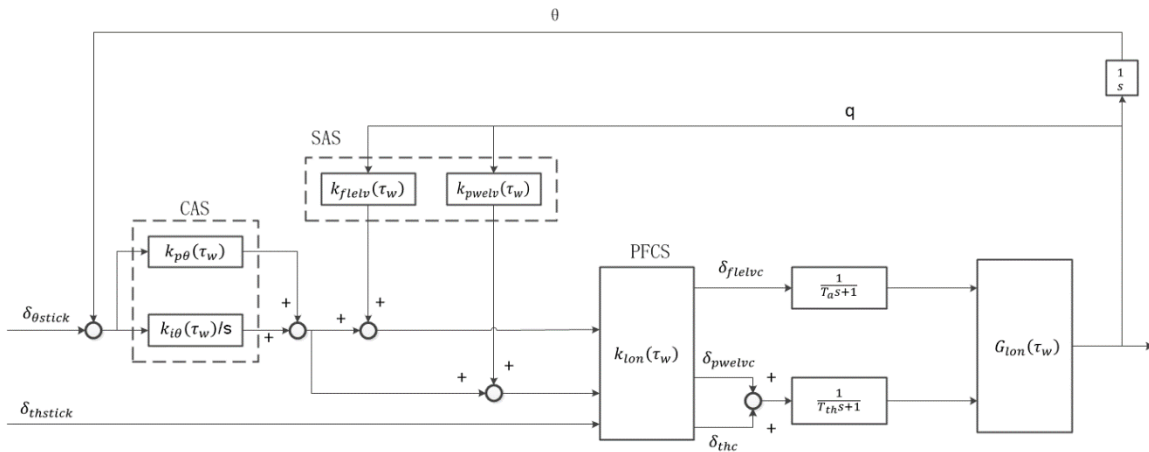


Figure 6. Longitudinal flight control law.

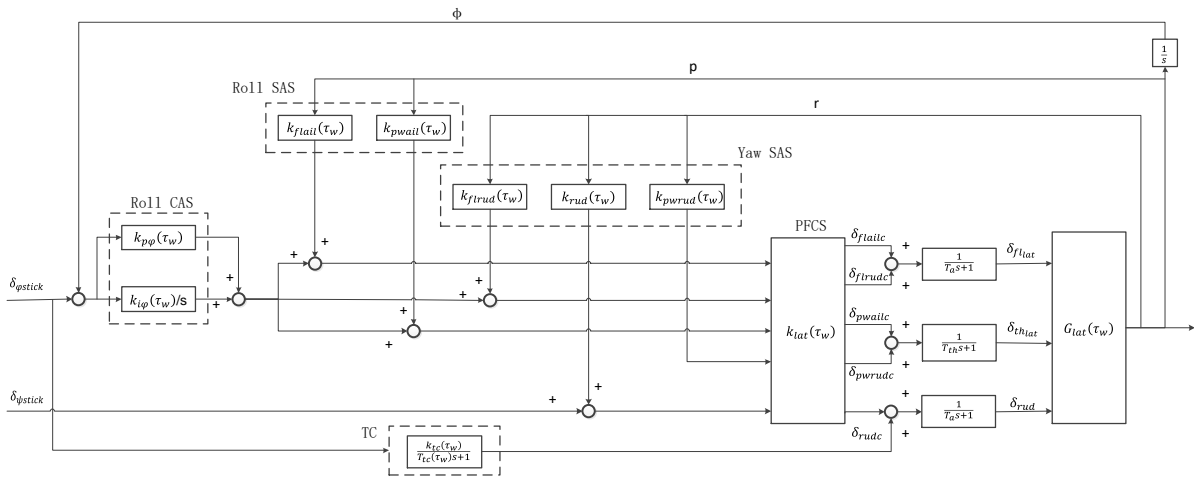


Figure 7 – Lateral & directional flight control law.

5. Virtual Flight Test

5.1 Test Setup

A four degree-of-freedom (DOF) virtual flight test rig (see Table 1 for technical index) is developed in the 1.4 m x 1.4 m Wind Tunnel, and then the virtual flight test is carried out.

Table 1 – Technical index of the 4-DOF virtual flight support device.

content	index
Pitch angle	$\pm 45^\circ$
Roll angle	$\pm 45^\circ$
Yaw angle	$\pm 180^\circ$
Vertical motion	≤ 100 mm
Maximum model weight	≤ 20 kg
Maximum model wing span	≤ 1000 mm
Maximum test wind speed	≤ 40 m/s

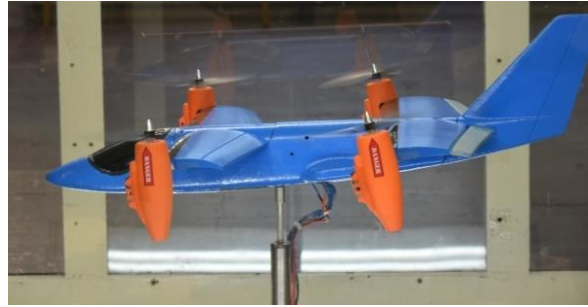
The overall layout of the virtual flight test system [10] in the field is shown in Figure 8. The QTR UAV is supported at the center of test section with the 4-DOF rig; the onboard sensors, motors and actuators are connected to the flight control system outside the wind tunnel by wire; For convenience of testing and manipulation, the ground station, including flight computer, visual display system and pilot stick, is placed at the rear side of test section.



Figure 8 – Layout of the apparatus in the wind tunnel.

5.2 Results and Discussion

The effectiveness of the flight control law is verified through the virtual flight test in wind tunnel for VTOL, fixed-wing and transition modes, respectively. The control gain parameters are optimized and the control stability characteristics of each mode are preliminarily evaluated. By virtual flight test simulating the full tilt-transition process, the validity of the tilt-transition corridor design method and control strategy is verified, as shown in Figure 9.



(a) VTOL mode



(b) tilt-transition mode



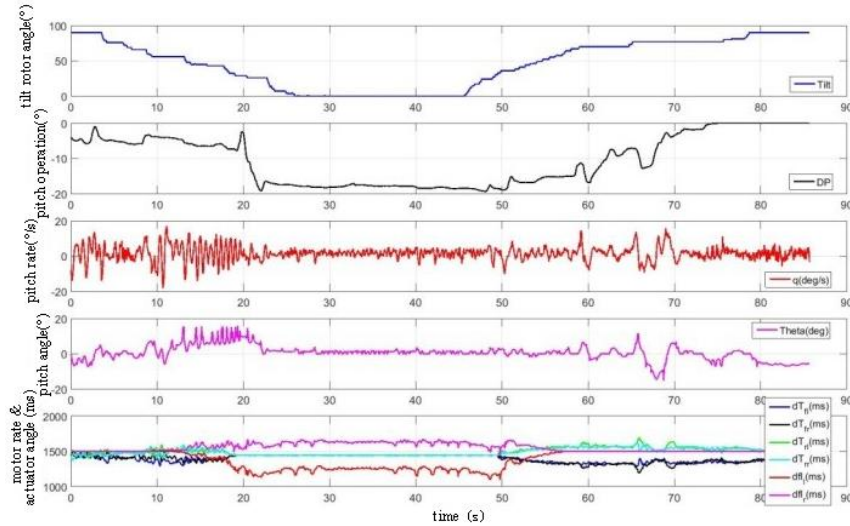
(c) fixed-wing mode

Figure 9 – Virtual flight test in wind tunnel with a tilt-rotor UAV.

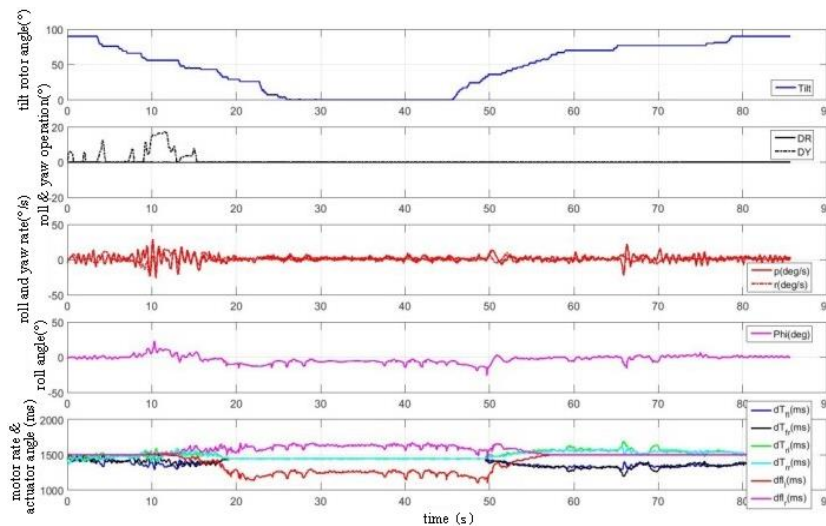
Take for example the full transition process, the key data log in virtual flight test is shown in Figure 10. The longitudinal control response is denoted by ‘(a)’ and lateral & directional one by ‘(b)’. The results show that the transition in “tilting corridor” is a continuous process including vertical take-off, accelerating transition, high speed cruise, decelerating transition, and vertical landing sequentially. At first, the vehicle hovers with the quadrotor configuration. Secondly, the wind speed rises from zero to the cruise speed; and the rotor tilt angle is adjusted to the corresponding value as wind speed increases according to the trimmed tilt corridor. Vertical motion and pitch movement are hardly seen, which means the flight can keep stable during the transition. Furthermore, when the wind speed becomes stable, the rotors face forward in the meantime and the flight turn into fixed-wing mode. Similarly, the decelerating transition performs with wind speed decreasing until the vehicle is recovered to quadrotor mode as the wind stops.

The test results indicate that: (1) The design method of the tilt transition flight corridor based on dynamic model trimming can ensure a safe and smooth transition between the two modes of the VTOL and high-speed forward flight. It provides a feasible solution of "slow-process" smooth switching between the VTOL mode and the fixed-wing level-flight mode of multi-rotor UAVs. (2) The flight dynamic model and flight control law, which are established based on gain schedule method, can automatically adjust their parameters according to the parameter of "rotor tilt angle" to satisfy the requirements of attitude stabilization control during different flight modes. (3) The virtual flight test in wind tunnel can effectively reduce the cost and risk of flight verification for tilt-rotor UAV and

its control strategy and control law, and greatly improve the efficiency of flight verification test.



(a) longitudinal control response



(b) lateral & directional control response

Figure 10 – Virtual flight test data log of tilt transition mode.

6. Conclusions

This paper focuses on a quad tilt rotor UAV with both the ability of VTOL and high speed cruise, briefly introduces the overall layout and flying mechanics, and formulates the model of flight dynamics for the three flight modes, including the VTOL mode, the transition mode and the fixed wing mode, with the same formation which takes the tilt angle of rotor as a variable. Following, the surface allocation, the tilt transition corridor and flight control law is designed, and the closed loop flight control system is constructed. At last, all the system is integrated in the virtual flight test in wind tunnel, which evaluates the augmentation effect and operation performance of the control laws in three flight modes, and preliminary validates the tilt transition corridor and its control scheme.

Acknowledgments

This work was partly supported by the Science and Technology Innovation 2030 Major Project under grant no. 2020AAA0104800 and the Natural Science Foundation of China under grant no.61903364.

Contact Author Email Address

mailto:niebowen_cardc@outlook.com

Copyright Statement

The authors confirm that they, and/or their company or organization, hold copyright on all of the original material included in this paper. The authors also confirm that they have obtained permission, from the copyright holder

of any third party material included in this paper, to publish it as part of their paper. The authors confirm that they give permission, or have obtained permission from the copyright holder of this paper, for the publication and distribution of this paper as part of the ICAS proceedings or as individual off-prints from the proceedings.

References

- [1] Gertler J. V-22 Osprey tilt-rotor aircraft: background and issues for congress. *CRS Report for Congress*, Congressional Research Service, 2011.
- [2] Johnson W. NDARC-NASA Design and Analysis of Rotorcraft-Theory. *NASA Technical Publication*, NASA Ames Research Center, NASA/TP-2015-218751, 2015.
- [3] Scully M. Adventures in low disk loading VTOL design. *NASA Technical Publication*, NASA Ames Research Center, NASA/TP-2018-219981, 2018.
- [4] Rothhaar P M, Murphy P C, Bacon B J, Gregory I M, Grauer J A, Busan R C, and Croom M A. NASA Langley distributed propulsion VTOL tiltwing aircraft testing, modeling, simulation, control, and flight test development. *14th AIAA Aviation Technology, Integration, and Operations Conference*, Atlanta, GA, AIAA Paper 2014-2999, 2014.
- [5] Muraoka K, Okada N, and Kubo D. Quad tilt wing VTOL UAV: aerodynamic characteristics and prototype flight test. *AIAA Infotech Aerospace Conference*, Seattle, Washington, AIAA Paper 2009-1843, 2009.
- [6] Sato M and Muraoka K. Flight controller design and demonstration of quad-tilt-wing unmanned aerial vehicle, *Journal of guidance, control, and dynamics*, Vol. 38, No. 6, pp 1071-1082, 2015.
- [7] Muraoka K, Okada N, Kubo D, and Sato M. Transition flight of quad tilt wing VTOL UAV. *28th Congress of the International Council of the Aeronautical Sciences (ICAS)*, Brisbane, Australia, ICAS Paper 2012-11.1.3, 2012.
- [8] Etkin B and Reid L D. *Dynamics of Flight: Stability and Control*. 3rd Edition, John Wiley and Sons Inc, Toronto, Canada, 1996.
- [9] Stevens B L, Lewis F L, and Johnson E N, *Aircraft Control and Simulation: Dynamics, Controls Design, and Autonomous Systems*, 3rd Edition, John Wiley and Sons Inc, Hoboken, New Jersey, 2015.
- [10] Guo L, Zhu M, Kong P, Nie B, Zhong C. Analysis of dynamic characteristics between prototype aircraft and scaled-model of virtual flight test in wind tunnel. *Acta Aeronautica et Astronautica Sinica*, Vol. 37, No. 8, 2583-2593, 2016 (in Chinese).